Journal of Microwaves, Optoelectronics and Electromagnetic Applications, Vol. 22, No. 1, March 2023
DOI: http://dx.doi.org/10.1590/2179-10742023v22i1265710

Notched Circular EBG based Circularly Polarized Antenna for Performance Enhancement

Alka Verma[1], Shilpee Patil[2], Anil Kumar Singh[3], Anil Kumar Pandey[4]
[1]*Department of Electronics & Communication Engineering, Teerthanker Mahaveer University, Moradabad, Uttar Pradesh, India, dralka.engineering@tmu.ac.in*
[2]*Department of Electronics & Communication Engineering, Galgotias College of Engineering & Technology, Greater Noida, India, shilpeepatil21@gmail.com*
[3]*Department of Electronics and Instrumentation Engineering, F.E.T, M.J.P. Rohilkhand University, Bareilly, Uttar Pradesh, India, anilei76@gmail.com*
[4]*Department of Electronics & communication Engineering, GL Bajaj Institute of Technology and Management, Greater Noida, Uttar Pradesh, India, anilpandey85@gmail.com*

***Abstract*—In this article, a novel Compact Circularly Polarized Antenna with a notched circular Electromagnetic Band Gap (NCEBG) structure is put forward. This proposed structure comprises of a truncated rectangular patch antenna having its ground plane defected by slots etched on it to achieve compactness and wide impedance bandwidth. Electromagnetic Band Gap structures have the attractive feature of in-phase reflection and stopband creation for surface waves, enabling the surface waves to be suppressed; this, in turn, leads to enhanced performance of the antenna when loaded with such structures. For enhancing the functioning of the antenna with regard to its impedance bandwidth, axial ratio bandwidth and gain, seven NCEBG's are etched on the substrate which surrounds the truncated patch. Additionally, the antenna proposed in this research exhibits compactness with a low profile of 0.473 λo x 0.473 λo x 0.039 λo (λo at center frequency of 7.46GHz represents free space wavelength). The measured outcomes of the prototype-fabricated antenna match well with the results of the simulation, showing 3-dB axial ratio bandwidth of 13.66% and an impedance bandwidth of 73.29% having a peak gain of 7.32dBi in the operating band. The improved functioning of the proposed antenna marks it as a favorable applicant for wireless communication techniques and thus finding its application in various ways.**

***Index Terms*—** Circularly polarized, Defected Ground Structure, Gain, Impedance Bandwidth, Notched Circular Electromagnetic Band Gap.

I. INTRODUCTION

The various field of wireless communication, which includes mobile communication, radio frequency identification (RFID) readers, wireless local area network (WLAN) applications, etc., there has been a rising demand for Circularly Polarized Antennas (CP antennas) to meet the constraint of compact, low profile, less costly antennas since they offer attractive features, such as flexibility of orientation of angle and reduction of multipath. To meet this demand, various methods such as perturbation, the introduction of asymmetrical slits, cutting slots on patch, loading parasitic shorting

Brazilian Microwave and Optoelectronics Society-SBMO *received 6 July 2022; for review 11 July 2022; accepted 26 Nov 2022*
Brazilian Society of Electromagnetism-SBMag

ISSN 2179-1074

elements, use of Defected Ground Structure etc. [1-5] have been used. One of the methods mentioned above is the Defected Ground Structure (DGS) method which has the attractive feature of repressing harmonics of a higher order, improving radiation of antenna by avoiding cross-polarization and preventing mutual coupling between elements lying close by. Various forms of DGS's, for example: cross-shaped [6], rectangular dumbbell [7], circular dumbbell [8] spiral [9], U in shape, V in shape [10] and H-shaped [11] have been reported. By using the aforementioned shapes of DGS, researchers have designed many circularly polarized antennas to accomplish a wide impedance as well as AR bandwidth. A.K Singh et al [12] designed a DGS-based annular ring CP antenna at 2.6GHz and achieved an impedance bandwidth of 34.61% with an AR bandwidth of 8.08%. Again, K. Wei et al [13] designed a CP antenna with its ground fractal defected and achieved 30MHz and 6MHz of impedance bandwidth and 3-dB axial-ratio bandwidth respectively. Although the performance of CP antenna-based on DGS improved, as reported in [14], it showed back radiation characteristics which limited the antenna's performance by 0.6 dB in terms of gain. To further enhance the operation of CP antennas by reducing back radiation as well as to achieve improvement in gain and efficiency, one of the methods adopted by researchers was the deployment of Electromagnetic Band Gap structures (EBG) [15]. Notably, these configurations are periodic/aperiodic artificial structures which introduce a particular stop band/pass band and counteract/aid the surface waves from propagating; this leads to improvements in antenna performance.

Various Electromagnetic Band Gap structures of different shapes, such as mushroom [16], dumbbell [17], spiral [18] etc., have been used to improve antenna performance. Upon use with a circularly polarized antenna, EBG depicted improved performance by reducing the surface waves. Many researchers have worked in this field and have used these structures as high impedance structures [19], metasurfaces [20], polarization-dependent EBG surfaces [21], etc. When implemented on antenna's ground plane, EBG structures showed an improved performance [22-24]. The attractive features of EBG structures has made these structures be used in broad area of applications in the antenna field. In microstrip antennas, EBG's enhances the performance of both linearly polarized as well as circularly polarized antennas. Notably, there are different ways to implement these structures on antennas. They can be implemented on antennas by being etched on the ground structure, surrounding the antenna's patch by such structures, or by being etched on substrate etc. By implanting in the ground structure a 4×4 annular-slot EBG, CP antenna of annular ring shape was fabricated in [25]; consequently, an enhanced 160MHz impedance bandwidth and AR bandwidth of 28MHz was achieved. In [26], a compact CP antenna employing EBG-based metasurface and meta-resonator was devised to enhance the antenna's operation. Later, numerous researchers executed EBG structures on the antenna by placing it around it and observed that while the antenna performance improved, it also resulted in an increase in size. Notably, by surrounding patch antenna loaded with an inclined slot with a mushroom-shaped EBG, Zhao et al [27] achieved wide axial bandwidth. To further enhance antenna's gain, researchers designed EBG based metasurface and placed it either above or below the

  ISSN 2179-1074

radiating patch [28-29]. In [30], a CP antenna with metasurface was proposed; here, four silts and a slot of L type achieved 18% and 12.8% of impedance bandwidth and AR bandwidth respectively. Again, a wideband Coplanar-waveguide fed CP antenna was fabricated in [31] with an inclined slot in ground plane and, upon placing a 2x2 U-shaped slot-loaded EBG-based metasurface on it, achieved an enhanced impedance bandwidth along with good AR bandwidth. Based on the above discussed literature survey, we conclude that EBG structures can enhance the performance of microstrip path antennas. With the aim to show improved performance that has not yet been reported, our proposed work implements a novel EBG structure on a circularly polarized DGS based antenna.

In our current research, we put forward a compact circularly polarized antenna in which the ground structure of the rectangular microstrip patch is integrated with rectangular slots to create a Defected Ground Structure (DGS) [32-33]. The substrate is loaded with seven notched circular Electromagnetic Band Gap (NCEBG) structures surrounding the patch. We carry out a nuanced parametric analysis by altering the dimensions of DGS and NCEBG; consequently, the final optimized results are attained. The antenna proposed in this work, in its operating band achieves 5750MHz of measured impedance bandwidth, AR bandwidth of 1100MHz with measured peak gain of 7.32dBi. This projected antenna is applicable in fixed-satellite service and mobile-satellite service covering 7900-8400MHZ.

II. UNIT CELL OF PROPOSED NCEBG STRUCTURE

Surface waves are observed on the interface among any two materials that are unrelated and could be metal and free space. Usually, these waves get bounded between the two aforementioned surfaces, causing their fields to decay exponentially [34] with reference to the perpendicular direction of the dissimilar surface. Surface waves in most antennas have been an issue because they lead to the propagation of radiation towards the ground surface in place of free space. EBG structures are materialized by implementation of dielectric, metallic, or composite structures. Two important and special electromagnetic properties are salient features of these structures. Of these two, the first is the stoppage of surface waves in specified frequency band known as the band gap while the second is the response of the phase when the plane wave illuminates the surface of EBG [35]. It was observed that the Electromagnetic Bandgap structures had a change in reflection phase on varying the frequency from 180º to -180º [36]. Apart from this, these configurations have several other enthusing traits, such as high impedance in their performance band. Given the presence of these characteristics, a significant amount of relevance has been stated, such as Transverse Electro Magnetic (TEM) waveguides, microwave filters and wire antennas of low profile [37]. Dielectric EBG structures have been put into application on microstrip antennas for performance enhancement by exhibiting a stop band in which surface waves are inhibited to be propagated. There are various methods to find the stop band; these are Reflection Phase diagram, Dispersion diagram and Direct Transmission method [38]. The method involved in our work is the Dispersion diagram method. Dispersion diagram refers to the plotting of propagation phase constant with frequency and is a vital characteristic of an EBG unit cell. Notably,

Brazilian Microwave and Optoelectronics Society-SBMO *received 6 July 2022; for review 11 July 2022; accepted 26 Nov 2022*
Brazilian Society of Electromagnetism-SBMag *ISSN 2179-1074*

the calculation was done by using a single EBG unit cell. From this unit cell, a periodic boundary condition [39], which has suitable phase shifts, was applied on various sides. The researchers observed that, based on the theorem of Floquet and its expansion by Bloch, the dispersion diagram showed periodic nature. As such, only one period was used to plot the graph of β-f for one particular period; this period is denoted the Brillouin zone. Within the Brillouin zone, the smallest area is a region in which symmetry was not related to directions. It is noteworthy that this region covers one-eighth of the complete Brillouin zone, expressed as Γ, X and M points [40-41].

In our current research, we fabricated a new EBG structure, shown in figure 1(a). This structure comprises a circular EBG with four notches on its circumference, with the length of each being r_1. These four notches are of thickness r_2-r_3, thus providing a wide band gap to the EBG structure. The relevant unit cell is implemented on our proposed antenna by etching seven such NCEBG cells on the substrate of the antenna. The band gap formation of our proposed notched circular EBG (NCEBG) depends on the unit cell dimensions and also on periodicity of the structure.

To calculate the stop band frequency, in this instance, we utilized the Bragg's condition [42] which states that the separation of the inter-cell, also referred as periodicity (a), is nearly equivalent to a half wavelength of the stop band central frequency. The calculation of EBG unit cell's size is done with reference to the Filling Factor (FF) and by using inter-cell separation.

The Filling factor is stated in (1).

$$FF = \frac{r_2}{a} \tag{1}$$

Here, FF is assumed to be 0.45 with 'a' as 5.3mm

Using the above equation, we get r_2=2.7mm

Notably, the central band gap frequency is calculated using (2) and (3):

$$a = \pi \beta \tag{2}$$

where, 'a' represents the periodicity of EBG pattern and π refers to the wavenumber of dielectric slab's

$$\beta = \frac{2\pi f_0 \sqrt{\epsilon_{re}}}{c} \tag{3}$$

where, f_o denotes the stop band center frequency

ϵ_{re} is effective dielectric constant of dielectric slab's

c is free space speed of light

To achieve the desired band gap, we get the measurements as shown in Table I after optimizing the dimensions of the NCEBG structure; this includes r_1, r_2 and r_3.

ISSN 2179-1074

TABLE I. DIMENSIONS OF UNIT CELL OF NCEBG

Parameter	**Magnitude (mm)**
Notch length, r_1	1.0
Radius of outermost circle, r_2	2.4
Radius of innermost circle, r_3	2.0

In the dispersion diagram method, the proposed unit cell EBG's frequency band gap is determined as shown in Fig. 1(b) using HFSS's Eigenmode solver. Irreducible Brillouin zone, which reflects periodicity and symmetry of unit cell having square lattice, is displayed in Fig. 1(c), to obtain dispersion diagram, irreducible Brillouin zone path is traced which is depicted in the expression below:

$$\Gamma\text{-X (Kx = 0°, Ky= 0°}\rightarrow\text{180°, X-M (Kx = 0°}\rightarrow\text{180°, Ky =180°), M- }\Gamma\text{ (Kx, Ky: 0°}\rightarrow\text{180°)} \quad (4)$$

where Kx is the phase offset in the x axis and Ky is the phase offset in the y axis.

It is seen that the band gap from the dispersion diagram lies between 4.64GHz and 10.91GHz, which is wideband, while the operating frequency bandwidth of our planned antenna also lies within the bandwidth of the proposed NCEBG structure.

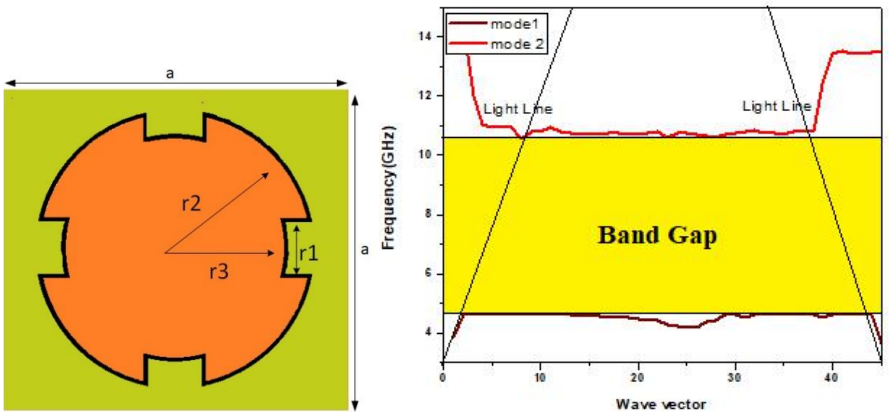

(a) (b)

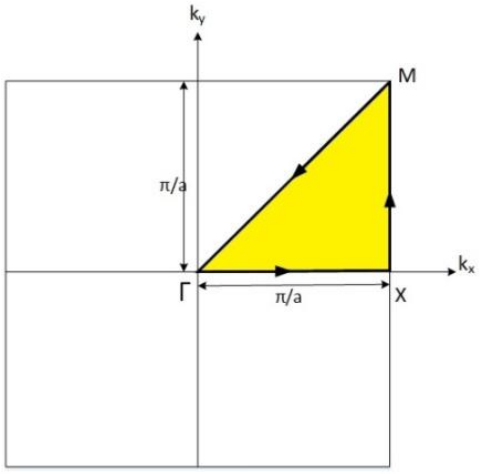

(c)

Fig. 1. Proposed Unit cell (a) Geometry (b) Dispersion diagram (c) Irreducible Brillouin zone for the square lattice unit cell.

Brazilian Microwave and Optoelectronics Society-SBMO *received 6 July 2022; for review 11 July 2022; accepted 26 Nov 2022*
Brazilian Society of Electromagnetism-SBMag

ISSN 2179-1074

III. DESIGN OF THE ANTENNA

Figs. 2(a), (b) and (c) depict our planned antenna from the top, bottom and side, respectively. This antenna comprises of a rectangular patch of dimensions L1 and W1, which has its adjacent corners truncated to dimension d. It is built on FR4 substrate comprising of thickness h having dielectric constant ($\in r$) of 4.4. An attractive feature of our proposed antenna is its compactness with defected ground plane (DGS) having dimensions Lg x Wg.

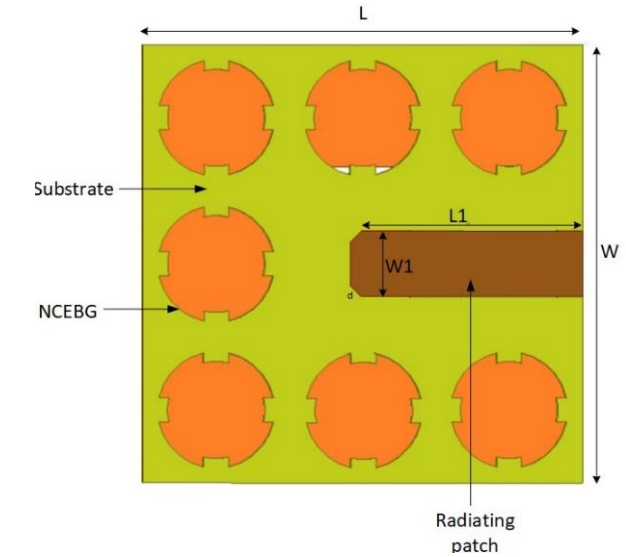

(a)

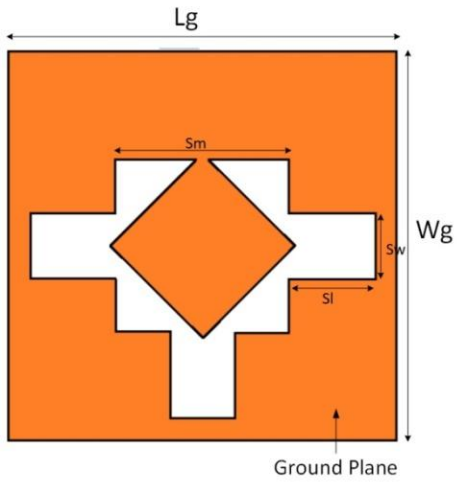

(b)

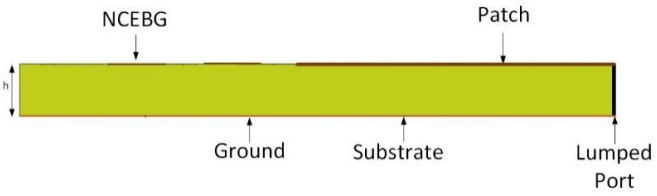

(c)

Fig. 2. The different views of proposed structure (a) Top view (b) Bottom view (c) Side view.

ISSN 2179-1074

The substrate is etched with seven notched circular EBG's surrounding the patch at a periodicity of 6 mm. Further, a lumped port is exploited to excite the antenna. Table II depicts the planned antenna's optimized dimensions.

TABLE II. PROPOSED ANTENNA 'S OPTIMIZED DIMENSIONS

Parameter	**Value**
Permittivityof FR4 as substrate, $\in_r$	4.4
Length of Substrate, L	18.0mm
Substrate Width, W	18.0mm
Thickness of substrate, h	1.6mm
Length of the patch, L_1	9.5mm
Patch Width, W_1	2.7mm
Truncated length, d	7.2mm
Ground plane length, Lg	18.0mm
Width of ground plane, Wg	18.0mm
Slot length in the ground plane, S_l	5.0mm
Slot width in the ground plane, S_w	3.0mm
DGS side length, S_m	7.9mm

IV. EVOLUTION OF PROPOSED ANTENNA

Development of the proposed antenna is depicted in figure 3 with the three following design steps: Antenna A, Antenna B and Antenna C (proposed antenna). Variation of return loss, axial ratio and gain with frequency for all the three aforementioned antennas are displayed in Figs. 4, 5 and 6 respectively, which indicate the process of evolution that led to the improved performance of our proposed antenna (Antenna C). Initially, Antenna A was designed by truncating two adjacent corners of a rectangular patch to generate the circularly polarized wave. As seen in figure 4, this antenna showed an impedance bandwidth of 22.64% (8.4GHz-10.42GHz). Also, narrow AR bandwidth of 1.04% (9.5GHz-9.6GHz) and poor gain is observed in Figs. 5 and 6, respectively. To further improve the antenna characteristics, the ground plane was defected with rectangular slots, thus disturbing the flow of current in it; eventually, this paved the way to the evolution of antenna B. The DGS is represented as an LC resonant circuit which shows band-stop characteristics, preventing higher harmonics while also averting the propagation of surface waves, thus effectively resulting in a reduction of overall losses. Figs. 4 and 5 show that upon implementation of DGS, the impedance bandwidth increases to 55.47% (6.07GHz – 10.73GHz); notably, center frequency of 8.4GHz and 3-dB AR bandwidth to 5.53% (8.26 GHz - 8.73 GHz) are achieved, respectively. From Fig. 7, it can be discerned that since DGS shows back radiation characteristics, Antenna B achieves poor gain in the AR bandwidth. In turn, this causes a reduction in gain [43-44]. To overcome this shortcoming, a novel EBG structure is etched on the substrate to further prevent the surface waves and, thereby, enhancing the radiation characteristics. [45-46]. The substrate is loaded with seven notched circular EBG's surrounding the truncated patch. From Fig. 6, it is observed that there is an improvement in the antenna's in the 3-dB ARBW ranging from 1.33dBi to 1.56dBi. Again, as depicted by Figs. 4 and 5, a wide return loss bandwidth and AR bandwidth of 65.68% (5.01GHz - 9.91GHz) and 13.33%

received 6 July 2022; for review 11 July 2022; accepted 26 Nov 2022

ISSN 2179-1074

(7.82GHz - 8.94GHz), respectively, is achieved. Thus, on observing the above stages of evolution, it is established that upon implementation of the Notched circular electromagnetic band gap structure, the overall performance improves; this is depicted in Table III.

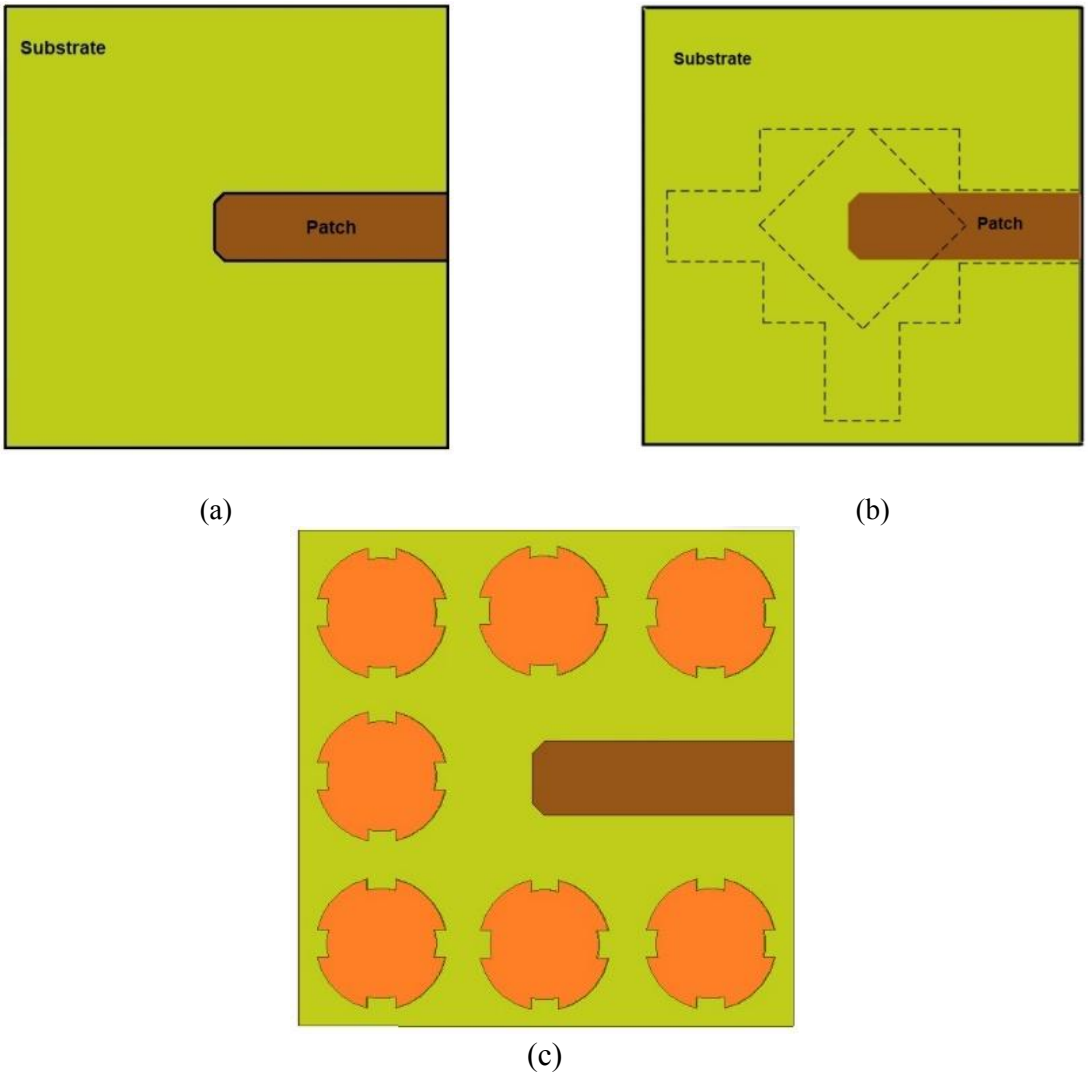

Fig. 3. Proposed antenna's evolution process: (a) Antenna A (b) Antenna B (c) Antenna C.

TABLE III. PARAMETERS OF ANTENNA A, B, AND C

Parameters	**Antenna A**	**Antenna B**	**Antenna C (Proposed)**
Impedance Bandwidth (MHz)	2020	4660	4900
Axial Ratio Bandwidth (MHz)	100	470	1120
Peak Gain (dBi) in the 3-dB axial ratio Bandwidth	0.15	0.25	5.48

ISSN 2179-1074

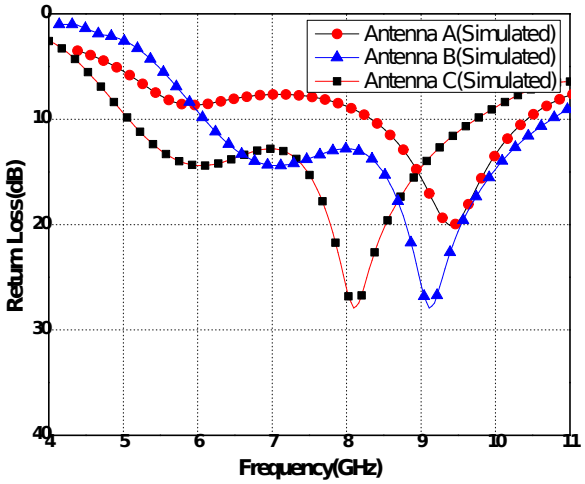

Fig. 4. Simulated Return Loss for different Antenna's: A, B and C.

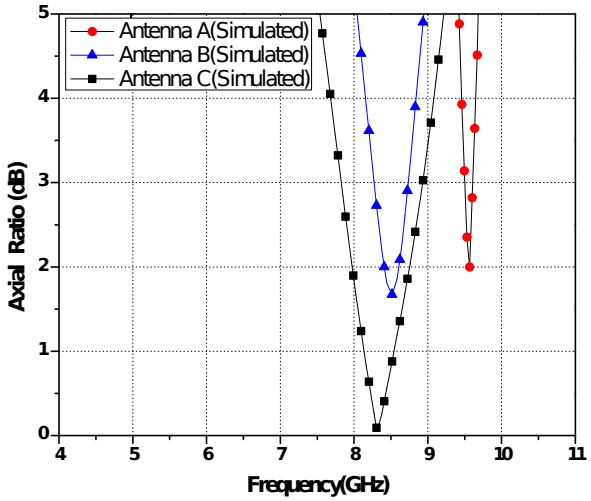

Fig. 5. Simulated Axial Ratio for different Antenna's: A, B and C.

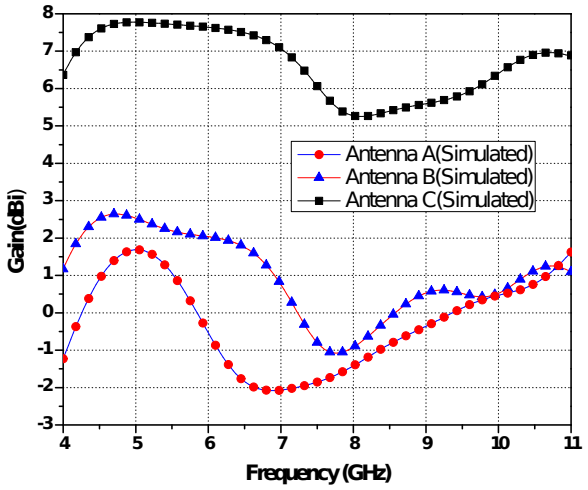

Fig. 6. Simulated Gain for different Antenna's: A, B and C.

received 6 July 2022; for review 11 July 2022; accepted 26 Nov 2022

ISSN 2179-1074

V. PARAMETRIC STUDY

For getting optimized dimensions of the antenna, we propose that parameters such as the radius of EBG and dimensions of the slots of DGS are varied; also the effect of these parameters on return loss graph and AR are analyzed and considered below. While performing the parametric operation, one of the parameters is selected to be analyzed while others are held constant.

A. Parametric analysis on r_2

From Fig. 7(a), it is observed that as we increase the parameter r_2, which is the outer radius of the EBG unit cell from 2.3 mm to 2.5mm, the resonant frequency increases with a decrease in the impedance bandwidth. Again, from the axial ratio characteristic in Fig. 7(b), we observed that at 2.4mm, the axial ratio value is minimum with a value of 0.05dB as compared to 2.3mm and 2.5mm, which have values of 0.28dB and 0.26dB, respectively. Thus, the analysis of the three aforementioned dimensions of r_2 optimizes its value to 2.4mm, while attempting to get better axial ratio value and wide impedance bandwidth.

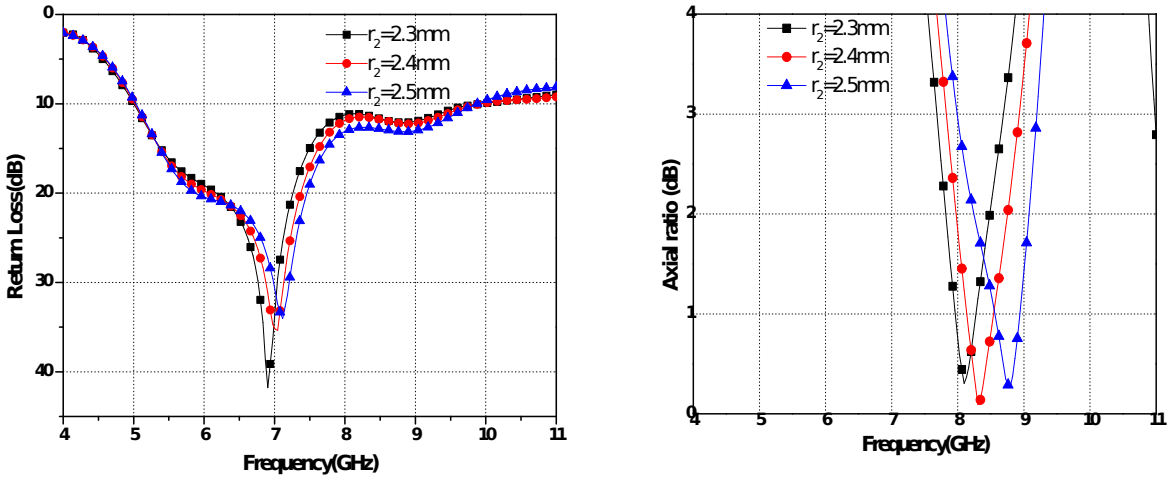

Fig. 7. (a) Effect on varying simulated return loss for various magnitude of r_2, (b) Effect on varying simulated axial ratio for various magnitude of r_2.

B. Parametric analysis on S_l

One dimension of the DGS is S_l, which is slot side length. On varying it from 4.8mm to 5.2mm, it is observed from Figs. 8(a) and 8(b) that S_l influences the return loss traits and axial ratio of the antenna. From Fig. 8(a), it is depicted that when S_l is 5mm, a maximum return loss bandwidth of 4900MHz is obtained in comparison to 4.8mm and 5.2mm, where the impedance bandwidth decreases to 4660MHz and 2990MHz, respectively. Fig. 8(b) shows that when S_l is 4.8mm and 5.2mm, the axial ratio deteriorates to 0.55dB and 0.25dB, respectively. In contrast, at S_l =5mm, the axial ratio reaches 0.05db, a value near to the standard value of one. Thus, we select the magnitude of S_l as 5mm to proceed with the final simulation of our proposed antenna.

ISSN 2179-1074

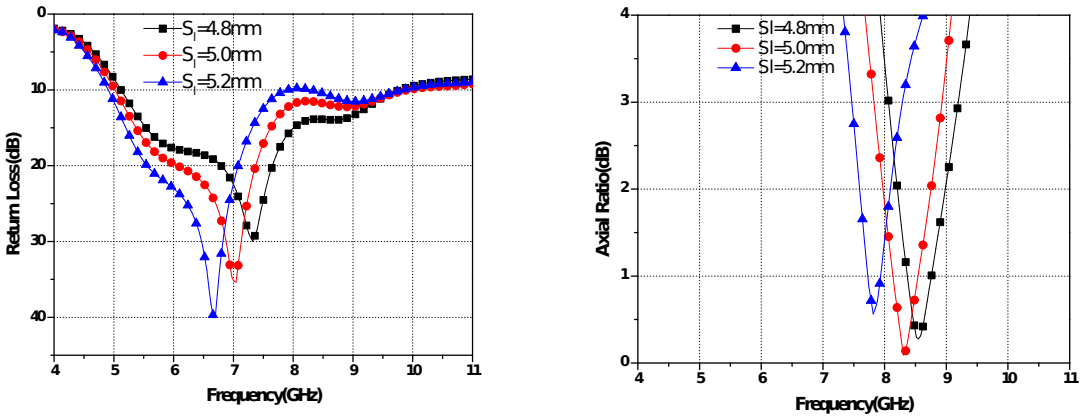

Fig. 8. (a) Effect on simulated return loss for various magnitude of S_l, (b) Effect on simulated axial ratio for various magnitudes of S_l.

VI. RESULTS AND DISCUSSION

By taking assistance of the Agilent Vector Network Analyzer (N5230A: PNA-L), the experimental results was obtained and near adherence to the results of simulation was observed. Because of fabrication tolerances and measurement system errors, a minute variation among the measured and simulated results is depicted.

On the ground plane, the surface current density (simulated result) at 8.31GHz is portrayed in Fig. 9 at the four values of θ which are 0°, 90°,180° and 270°. It clearly indicates that when θ attains value of 0° and 180°, the vector currents (simulated) are in phase opposition having their magnitude equal. Likewise, when θ is 90° and 270°, they are of same magnitude but in phase opposition. Therefore, it is perceived that on change in phase, rotation of vectors is in anticlockwise direction and, thus, it can be determined that proposed structure depicts left-hand circular polarization (LHCP). It is also observed that the orthogonal mode is TM11 mode, which is excited by using lumped port excitation.

Fig. 10, depicts measured and simulated return loss versus the frequency of the CP antenna with NCEBG is depicted. It is discerned that the proposed structure gives a simulated impedance bandwidth of 65.68% (5.01GHz to 9.91GHz) at center frequency of 7.46 GHz with measured impedance bandwidth of 73.29% (4.97 GHz to 10.72 GHz). Again, from Fig. 11, it is observed that a wide AR bandwidth of 13.36% (7.82GHz-8.94GHz) is obtained at the center frequency of 8.38GHz with the measured AR bandwidth as 13.66% (7.50GHz-8.60GHz) having minimum axial ratio of 0.08dB, showing that a pure circular polarization is obtained. Next, Fig. 12 shows the inset image of our fabricated proposed antenna, which achieves a peak gain (measured) of 7.32dBi in the operating bandwidth with a peak gain (measured) in AR bandwidth of 5.12dBi. Thus, it is predicted that on implementation of NCEBG, the surface waves are suppressed, which, in turn, results in enhancement of gain.

ISSN 2179-1074

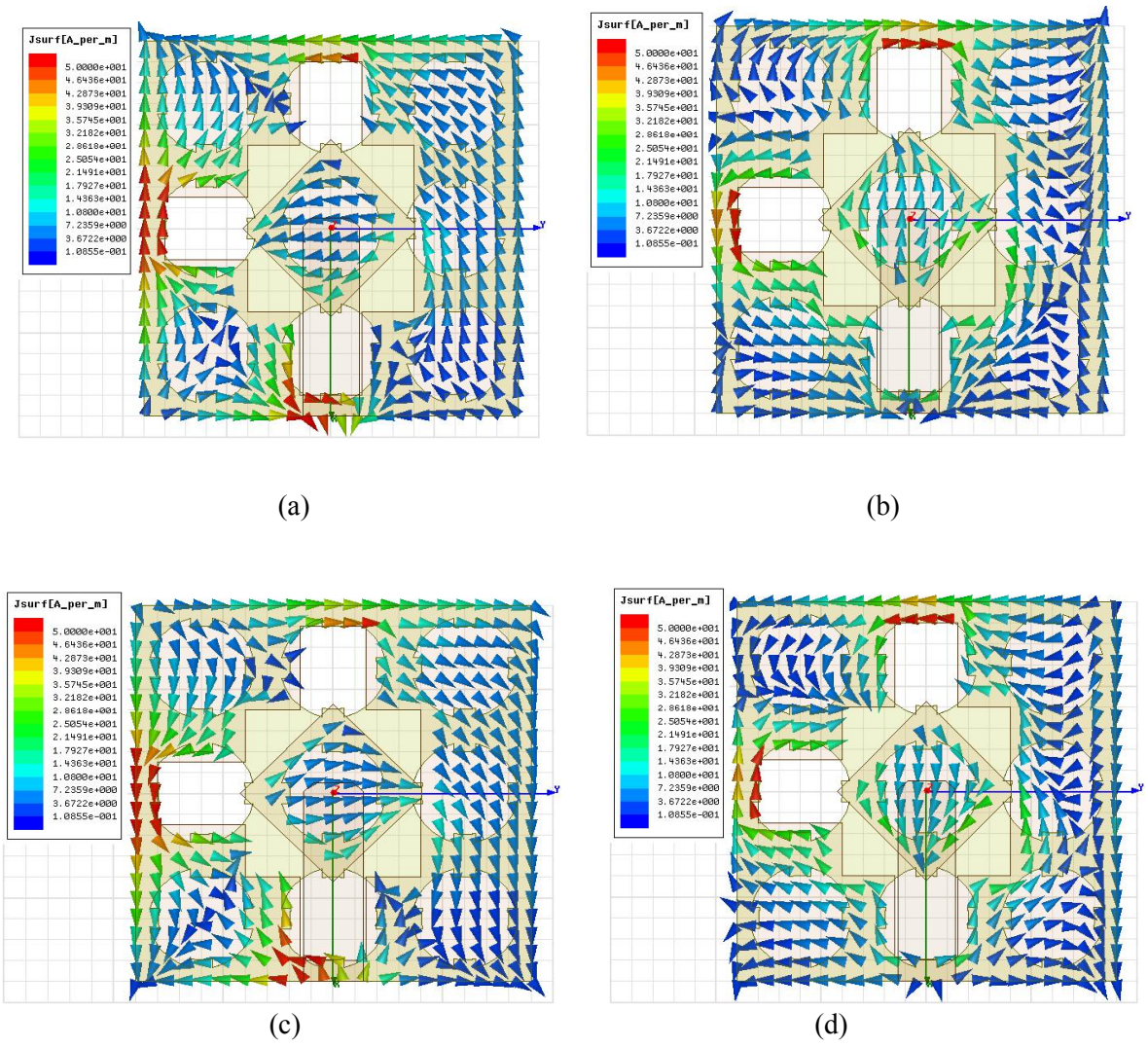

Fig. 9. Illustration of Surface current density at different value of θ . (a) 0° (b) 90° (c) 180° (d) 270°.

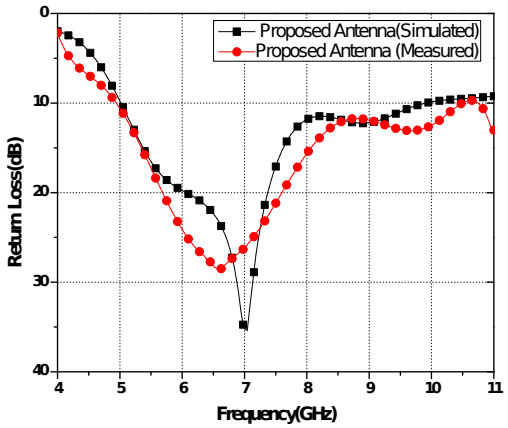

Fig. 10 Return loss bandwidth with frequency.

received 6 July 2022; for review 11 July 2022; accepted 26 Nov 2022

ISSN 2179-1074

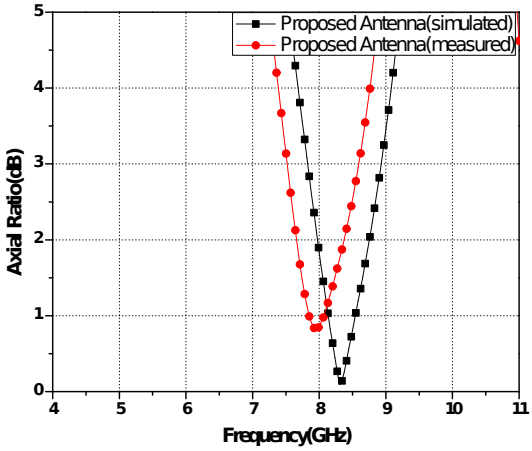

Fig. 11. AR bandwidth with frequency.

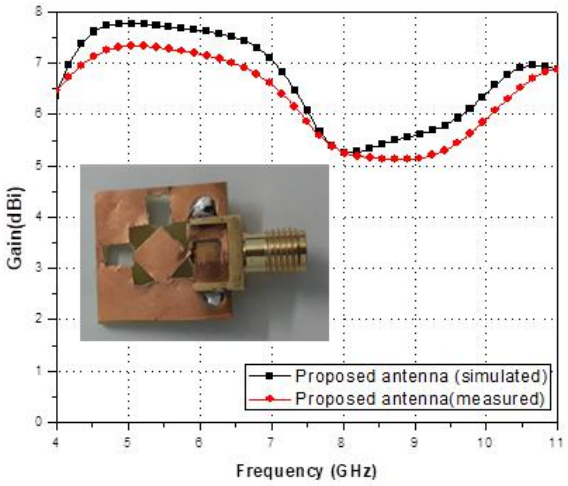

Fig. 12. Gain with frequency (Inset: Fabricated Antenna).

The antenna observes a good LHCP radiation at 8.38GHz in the broadside. Fig. 13 displays the simulated and measured LHCP and RHCP radiation patterns in the two planes: x-z and y-z. Both results, measured as well as simulated, agree well and in the two planes, the 3dB beamwidths are 52° and 68°, respectively. The 3D radiation pattern at 8.38GHz is shown in Fig. 14. Following this, Table 4 depicts our planned antenna in contrast with other reported EBG based CP antennas present in the survey, showing that our antenna is more compact with improved performance.

received 6 July 2022; for review 11 July 2022; accepted 26 Nov 2022

ISSN 2179-1074

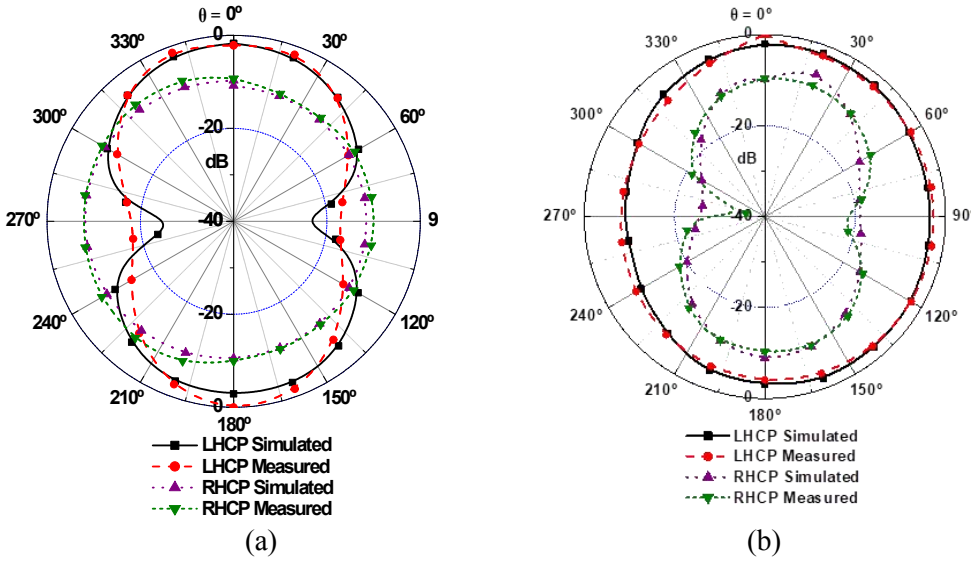

Fig. 13. At 8.38GHz the measured and simulated radiation pattern (a) X-Z plane, (b) Y-Z plane.

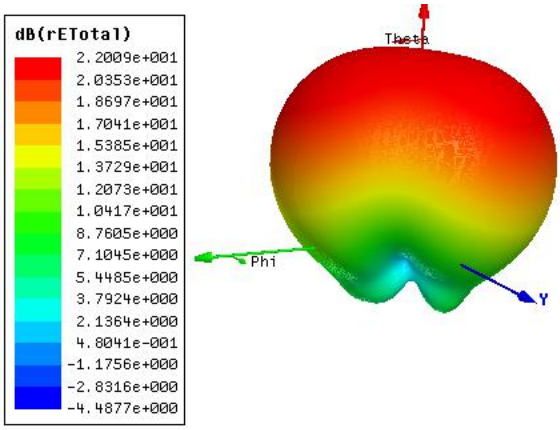

Fig. 14. 3D radiation pattern at 8.38GHz.

TABLE IV. COMPARATIVE SURVEY OF THE CITED EBG BASED CP AS COMPARED TO OUR PLANNED ANTENNA

Ref.	Size of Antenna(λ_o^3)	Feed Technique	Dielectric constant of the substrate	Measured Impedance Bandwidth (GHz)	Measured 3-dB AR Bandwidth (GHz)	Gain (dBi)
[25]	0.78x0.78x0.009	Coaxial Probe	4.1	1.681 to 1.841 (9.08%)	1.798 to 1.826 (2.80%)	4.2
[26]	0.435x0.435x0.02	Coaxial Probe	2.65	2.930 to 3.180 (8.18%)	2.990 to 3.090 (3.3%)	5.9
[27]	0.897x0.897x0.009	Coaxial Probe	4.4	2.349 to 2.477 (5.31%)	2.41 to 2.441 (1.28%)	7.5
[30]	0.865x0.865x0.038	Coaxial Probe	3.5	5.110 to 6.120 (18%)	5.35 to 6.08 (12.8%)	6.9
[31]	0.034x0.034x0.037	Coplanar Waveguide	4.4	2.82 to 4.00 (34.6%)	3.135 to 3.354 (6.8%)	3.9
Proposed	0.473x0.473x0.038	Lumped Port	4.4	4.97 to 10.72 (73.29%)	7.50 to 8.60 (13.66%)	7.32

ISSN 2179-1074

VII. CONCLUSION

In this article, a notched Circular EBG based CP antenna suitable for fixed-satellite service and mobile-satellite service covering 7900-8400MHz has been designed. The proposed antenna has measured impedance bandwidth and axial ratio bandwidth as 73.29% and 13.66% respectively with peak gain of 7.32dBi. The designing of the proposed notched Circular EBG has been studied in detail and parametric studies of the proposed NCEBG based CP antenna are carried out to generate results that may be helpful for designing EBG based antenna in the future.

REFERENCES

[1] S. Baudha, V.D Kumar, "Corner Truncated Broadband Patch Antenna with Circular Slots," Microwave and Optical Technology Letters, vol.57, pp,845-848, February, 2015.
[2] V.D Lam, K. M. Luk, K.F Lee, H. Wong and K.B. Ng, "Small Circularly Polarized U-Slot Wideband Patch Antenna," IEEE Antennas and Wireless Propagation Letters, vol.1, pp. 87-90, Febuary,2011.
[3] N. Nasimuddin, X. Qing and Z. N. Chen, "Compact Asymmetric-Slit Microstrip Antennas for Circular Polarization," IEEE Transaction on Antenna and Propagation, vol. 59: 285-288, January,2011.
[4] K. K. So, K. B. Ng, K. M. Luk, C. H. Chan, Q Xue, "Virtually Shorted Patch Antenna for Circular Polarization," IEEE Antenna sand Wireless Propagation Letters, Vol. 9, pp. 1213-1216, February, 2010.
[5] S. Patil, A.K. Singh. V. K Pandey, B.K Kanaujia and A.K Pandey, "A Simple and Compact Broadband Circularly Polarized Circular Slot Antenna for WLAN/Wimax/DBS Applications," Frequenz,Vol. 76, pp 209-219, April, 2021.
[6] D. Guha, S. Biswas, M. Biswas, J.Y. Siddiqui, and Y. M. M. Antar, "Concentric Ring-Shaped Defected Ground Structures for Microstrip Applications," IEEE Antennas and Wireless Propagation Letters, vol.5, pp.402-405, January 2003.
[7] C.S. Kim, J.S. Park, D. Ahn and J.B Lim, "A Novel 1-D Periodic Defected Ground Structure for Planar Circuits," IEEE Microwave and Wireless Component Letters, vol.10, pp.131-133, 2000.
[8] A.B. Abdel-Rahman, A. K Verma, A. Boutejdar and A.S. Omar, "Control of Bandstop Response of Hi-Lo Microstrip Low-Pass Filter Using Slot in Ground Plane," IEEE Transaction on Microwave Theory Technology, vol. 52, pp. 1008-1013, March 2004.
[9] C.S. Kim, J.S. Lim, S Nam, K.Y. Kang and D. Ahn, "Equivalent Circuit Modelling of Spiral Defected Ground Structure for Microstrip Line," Electronics. Letters, vol.38, pp.1109-1110, April 2002.
[10] D.J, "Novel U Slot and V-Slot DGSs for Bandstop Filter with Improved Q," IEEE Transaction on Microwave Theory Technology, vol.54, pp. 2840-2847, April2006.
[11] M.K. Mandal and S Sanyal. "A Novel Defected Ground Structure for Planar Circuits," IEEE Microwave and Wireless Component Letters, vol. 16: pp. 93-95, Febuary 2006
[12] A.K Singh, R.K Gangwar and B. K Kanaujia," Sectored Annular Ring Microstrip Antenna with DGS for Circular Polarization," Microwave and Optical Technology Letters, vol.58, pp.569-573, January 2016.
[13] K. Wei, J. Y Li, L. Wang, R. Xu and Z. J Xing, "A New Technique to Design Circularly Polarized Microstrip Antenna by Fractal Defected Ground Structure," IEEE Transaction on Antenna and Propagation, vol. 65(7) pp.3721–3725, May 2017.
[14] A. Ghosh, S. Chakraborty, S. Chattopadhyay, A. Nandi, B. Basu, IET Microw. Antennas Propag., Vol. 10, Iss. 1, pp. 68–78, 2016
[15] B. A. Munk, Frequency Selective Surfaces: Theory and Design. New York, NY, USA: John Wiley & Sons, 2000.
[16] Y. Dong, H. Toyao and T. Itoh, "Compact Circularly-Polarized Patch Antenna Loaded with Metamaterial Structure," IEEE Transaction on Antenna and Propagation, vol.59, pp.4329-4334, November, 2011
[17] A. Yu, "A Novel Method to Improve the Performance of Microstrip Antenna Arrays using Dumbbell EBG structures plane," IEEE Antennas and Wireless Propagation Letters vol. 2, pp.170-172, 2003.
[18] Z. Qiu-Rong, Y. Fu and N. C Yuan, "A Novel Compact Spiral Electromagnetic Band-Gap (EBG) structure," IEEE Transaction on Antenna and Propagation, vol.56, pp.1656 – 1660, August 2006.
[19] Y. Shen, "Minimized Low-Profile Wideband Antennas Using High Impedance Surface," International Journal of Antennas and Propagation,Vol. 2017, 1-12, September 2017.
[20] Y. Jia, Y. Liu, S. Gong, W. Zhang and G. Liao, "A low-RCS and High-Gain Circularly Polarized Antenna with a Low Profile, Applications," IEEE Antennas and Wireless Propagation Letters, vol.16, pp. 2477 – 2480,2017
[21] A. Verma, A.K. Singh, N., Srivastava, S. Patil and B. K. Kanaujia, "Circularly Polarized Microstrip Antenna using SLPD Electromagnetic Band Gap Structure applications," Frequenz, vol 74, pp.41-51, January 2020
[22] S. Pflaum, P. Thuc, G. Kossiavas and S. Robert, "Performance Enhancement Of Circularly Polarized Patch Antenna for Radio Frequency Identification Readers Using An Electromagnetic Band-Gap Ground Planes," Microwave and optical technology letters, vol.55. pp. 1599-1602 ,2013
[23] Q. Chen, H. Zhang, L. Yang, X. F Zhang and Z. Yi-Chao, "Wideband and Low Axial Ratio Circularly Polarized Antenna Using AMC-Based Structure Polarization Rotation Reflective Surface," International Journal of Microwave and Wireless Technologies, vol. 10(9), pp.1058-1064, 2016.
[24] A.S. Jalal and M. H. Jwair, "On the Performance of a Microstrip Antenna based UC-PBG structures for UHF RFID Readers," Engineering and Technology Journal, vol.36 pp.480-487, October 2018.

Brazilian Microwave and Optoelectronics Society-SBMO *received 6 July 2022; for review 11 July 2022; accepted 26 Nov 2022*
Brazilian Society of Electromagnetism-SBMag *ISSN 2179-1074*

[25] X. L. Bao G and M. J. Ruvio Amman, "A Circularly Polarized Annular-ring Patch Antenna with a Ground plane EBG Annular-slot Array," International journal of microwave and optical technology, vol. 69-75, 2008.
[26] H. X. Xu, GM Wang, J. G. Liang, M. Q. Qi and X. Gao, "Compact Circularly Polarized Antennas Combining Metasurfaces and Strong Space-Filling Meta-Resonators," IEEE Transaction on Antennas Propagation, vol.61, pp.3442−3450, 2013.
[27] Z.K Wang, X.H Yuan and B. Zhang B and G.Q Luo, "An Axial-Ratio Beam-Width Enhancement of Patch-Slot Antenna Based on EBG" Microwave and optical technology letters, vol. 59,493-496, January 2017.
[28] A. Verma, A. K. Singh, N. Srivastava, S. Patil and B. K. Kanaujia, "Performance Enhancement of Circularly Polarized Patch Antenna Using Slotted Circular EBG-Based Metasurface," Frequenz, 75(1-2), 35–4, October 2020.
[29] A. Verma, A. K. Singh, N. Srivastava, S. Patil and B. K. Kanaujia, "Hexagonal Ring Electromagnetic Band Gap based Slot Antenna for Circular Polarization and Performance Enhancement," Microwave Optical and Technology and Letters, vol. 62, no 7, pp.2576-2587,2020.
[30] L Zhipeng, J. Ouyang and F. Yang, "Low-Profile Wideband Circularly Polarized Single-Layer Metasurface Antenna," Electronics letters, vol.54, pp.1362–1364,2018.
[31] A. Verma, A. K Singh, N. Srivastava, S. Patil and B. K Kanaujia," Slot Loaded EBG-based Metasurface for Performance Improvement of Circularly Polarized Antenna for WiMAX Applications," International Journal of Microwave and Wireless Technologies, vol.12, pp.212-220, September 2019.
[32] D. M. N. Elsheakh, H. A. Elsadek, and E. A. Abdullah, Antenna Designs with Electromagnetic Band Gap Structures, Metamaterial. InTech, Rijeka, Croatia, 2012.
[33] G.-H. Li, X.-H. Jiang, and X.-M. Zhong, "A novel defected ground structure and its application to a lowpass filter," Microw. Opt. Technol. Lett., vol. 48, no. 9, pp. 1760–1763, 2006.
[34] F. R. Yang, K. P. Ma, M. Y. Qian, and T. Itoh, "A uniplanar compact photonic-bandgap (UC-PBG) structure and its applications for microwave circuits," IEEE Transactions on Microwave Theory and Techniques, vol. 47, no. 8, pp. 1509–1514, 1999.
[35] E. Yablonovitch, "Inhibited spontaneous emission in solid-state physics and electronics," Phys. Rev. Lett., vol. 58, no. 20, pp. 2059–2062, 1987.
[36] F.Yang, Y. Rahmat-Samii,"Microstrip antennas integrated with electromagnetic (EBG) structures: a low mutual coupling design for array applications," *IEEE Trans. Antennas Propag.* Vol.51, pp.2936– 2946, 2003.
[37] F. Yang, Y. Rahmat-Samii," Electromagnetic Band Gap Structures in Antenna Engineering," Cambridge. U.K.: Cambridge Univ. Press, 2009.
[38] P. Samineni, T. Khan and A. De, "Modeling of electromagnetic band gap structures: A review", Int. J. RF Microw. Comput.-Aided Eng., vol. 27, no. 2, pp. e21055, 2017.
[39] D. Sievenpiper, Lijun Zhang, R. F. J. Broas, N. G. Alexopolous and E. Yablonovitch, "High-impedance electromagnetic surfaces with a forbidden frequency band," in IEEE Transactions on Microwave Theory and Techniques, vol. 47, no. 11, pp. 2059-2074, Nov. 1999.
[40] Y. Lee, Y. Junho and Raj Mittra. "Investigation of electromagnetic bandgap (EBG) structures for antenna pattern control," IEEE Antennas and Propagation Society International Symposium. Digest. Held in conjunction with: USNC/CNC/URSI North American Radio Sci. Meeting vol.2,(Cat. No.03CH37450) 2, pp.1115-1118, 2003.
[41] E. Zbay, A. Abeyta, and G. Tuttle, "Measurement of a three-dimensional photonic band gap in a crystal structure made of dielectric rods," Physical Review B, vol. 50, no. 3, pp. 1945–1948, 1994.
[42] Lombardet, B., L.A. Dundas, R. Ferrini, and R. Houdre, "Bloch Wave Propagation in two Dimensional Photonic Crystals: Influence of Polarization," *Optical and Quantum Electronics* 37, 293-307, 2005
[43] G.-H. Li, X.-H. Jiang, and X.-M. Zhong, "A novel defected ground structure and its application to a lowpass filter," Microw. Opt. Technol. Lett., vol. 48, no. 9, pp. 1760–1763, 2006.
[44] C. S. Kim, J. S. Lim, S. Nam, K. Y. Kang, and D. Ah (2002) Equivalent circuit modelling of spiral defected ground structure for microstrip line. *Electronics Letters*, vol. 38, no. 19, pp. 1109–1110, 2002.
[45] A. S. Barlevy and Y. Rahmat-Samii, "Characterization of electromagnetic band-gaps composed of multiple periodic tripods with interconnecting vias: concept, analysis, and design," IEEE Trans. Antennas Propag., vol. 49, no. 3, pp. 343–353, 2001.
[46] L. Liang, C. H. Liang, L. Chen, and X. Chen, "A novel broadband EBG using cascaded mushroom-like structure," Microw. Opt. Technol. Lett., vol. 50, no. 8, pp. 2167–2170, 2008

received 6 July 2022; for review 11 July 2022; accepted 26 Nov 2022

ISSN 2179-1074